# Biochemical and genetic evidence for the presence of multiple phosphatidylinositol- and phosphatidylinositol 4,5-bisphosphate-specific phospholipases C in *Tetrahymena*

George Leondaritis, Theoni Sarri, Ioannis Dafnis, Antonia Efstathiou, and Dia Galanopoulou

## Supplemental Figures, Legends and Tables

**Fig S1**

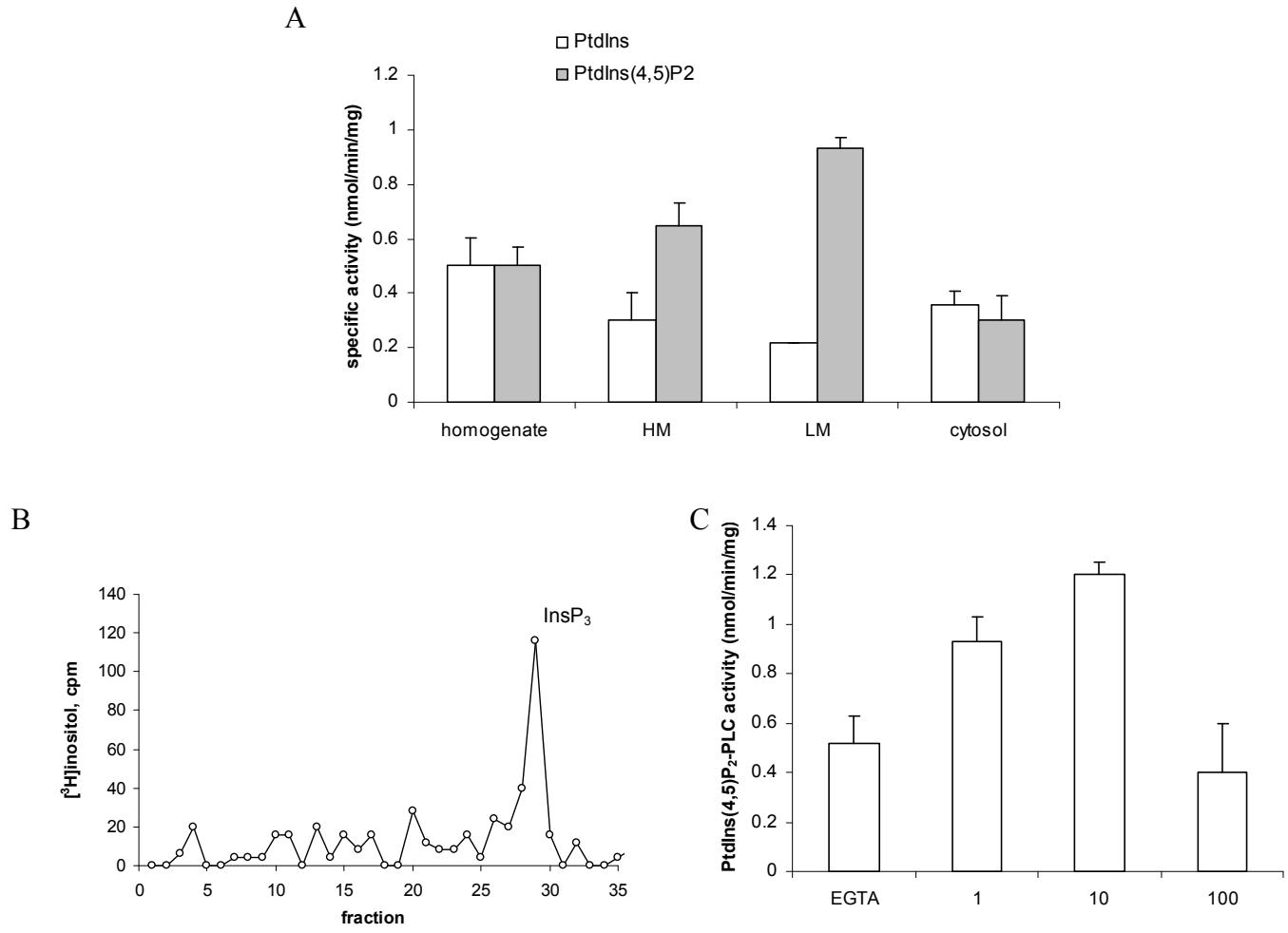


**Supplemental Fig. 1.** Phosphoinositide-hydrolyzing activities of *T. thermophila* CU438.1. (A) [$^3$H]PtdIns and [$^3$H]PtdIns(4,5)$P_2$-hydrolyzing activities were determined in homogenate and subcellular fractions (HM, heavy membrane; LM, light membrane) as described for Fig. 1A with the exception that for PtdIns, EGTA was added at 3 mM. Note that PtdIns-hydrolyzing activity in the absence of $Ca^{2+}$ is higher in the homogenate fraction and that PtdIns(4,5)$P_2$-hydrolyzing activity predominates in LM fraction. Data represent means ± SD of the results from three independent experiments, each assayed in duplicate. (B) [$^3$H]inositol-labeled water soluble products of PtdIns(4,5)$P_2$-hydrolyzing activities of LM fraction, were subjected to chromatography on Dowex AG-1x8, as described for Fig. 1C. $InsP_3$ is the major product of PtdIns(4,5)$P_2$ hydrolysis indicating a PI-PLC activity. (C) *T. thermophila* LM fraction PtdIns(4,5)$P_2$-PLC is activated by low micromolar $Ca^{2+}$ concentrations. PtdIns(4,5)$P_2$-PLC activity was assayed in the presence of the EGTA 3mM or in the presence of the indicated free $Ca^{2+}$ μM concentrations. Data represent means ± SEM of the results from two independent experiments, each assayed in duplicate.

**Fig. S2**

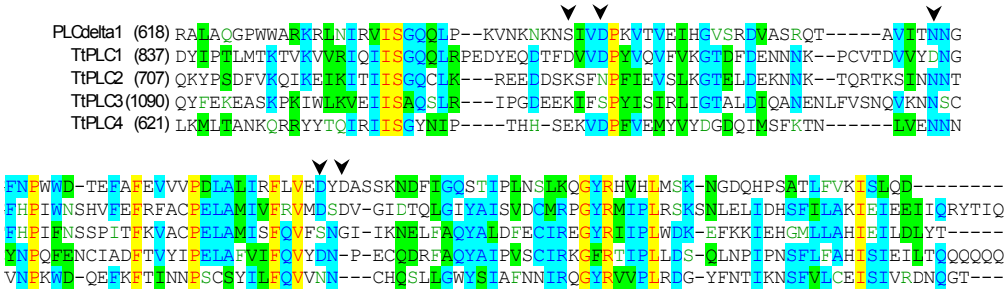


**Supplemental Fig. 2A.** Sequence alignment of the C2 domains from *T. thermophila* PLCs and human PLCδ1. The alignment was modelled on the PI-PLCδ1 C2 domain. Arrowheads indicate the position of residues in PLCδ1-C2 domain that may function as $Ca^{2+}$-binding sites (retrieved from the NCBI-BLAST domain database). Note that critical Asp or Asn residues are primarily conserved in Tt*PLC1* as compared to Tt*PLC2* and Tt*PLC3*/*PRIP*.

**Fig. S2 (continued)**

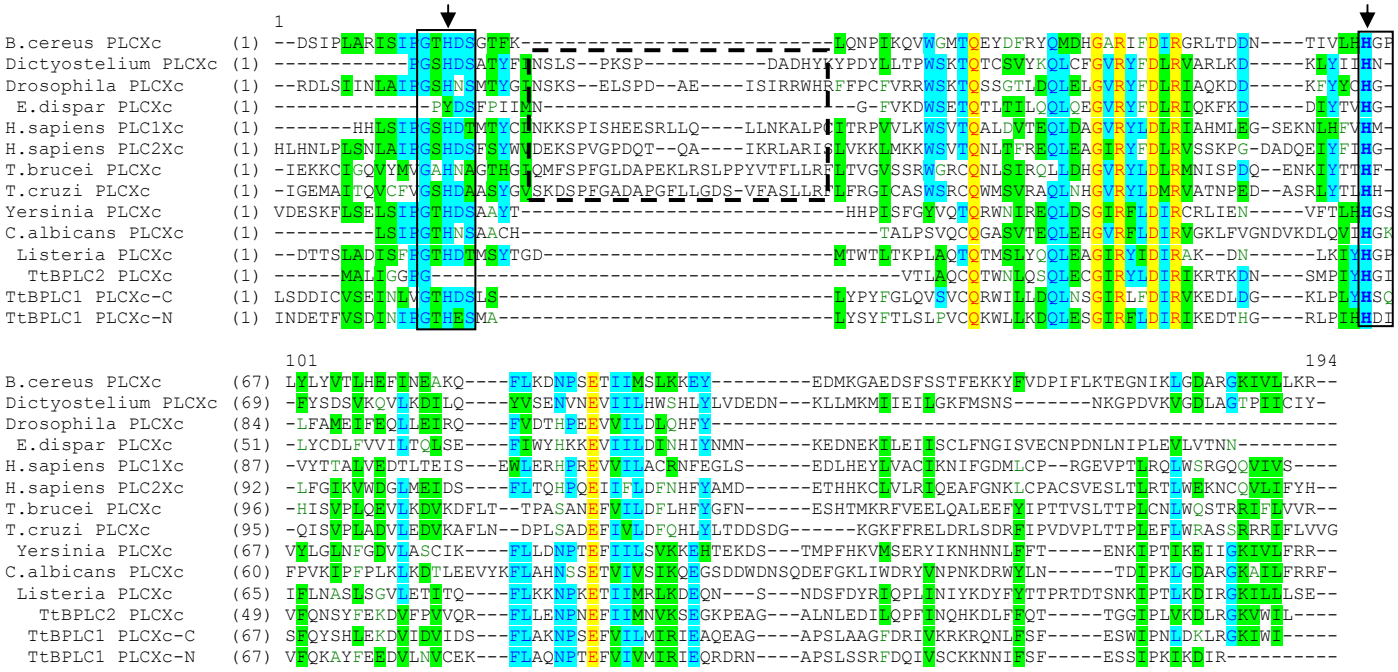


**Supplemental Fig. 2B.** Sequence alignment of the PLCXc domains from bacterial PLCs. Accession numbers for PLCs are listed in Supplemental Table 2. Domain boundaries were retrieved from the SMART database. The alignment was modelled on the *B. cereus* PtdIns-PLCXc domain. Arrows and the corresponding boxes indicate the position of catalytic His residues (His32 and His82 in *B. cereus* PLC). Note that: (i) all Group II PtdIns-PLCs have trypanosome-like insertions of approx. 25 amino acids (in *T. brucei*) between β-strand I and α-helix 1′ of the PLCXc structure indicated by a dotted box (ref. 17 in the manuscript); (ii) the alignment has been manually adjusted to correctly position the second catalytic His residue of Group II PtdIns-PLCs (shown in bold face). Mis-alignment of this catalytic His in Group II PtdIns-PLCs results in their annotation as "inactive PLCs" in some databases; (iii) *Entamoeba dispar* PLC and Tt*BPLC2* apparently lack the first catalytic His residue; (iv) Tt*BPLC1* PLCXc-C and -N correspond to the C- and N-terminal PLCXc domains, respectively.

**Fig. S2 (continued)**

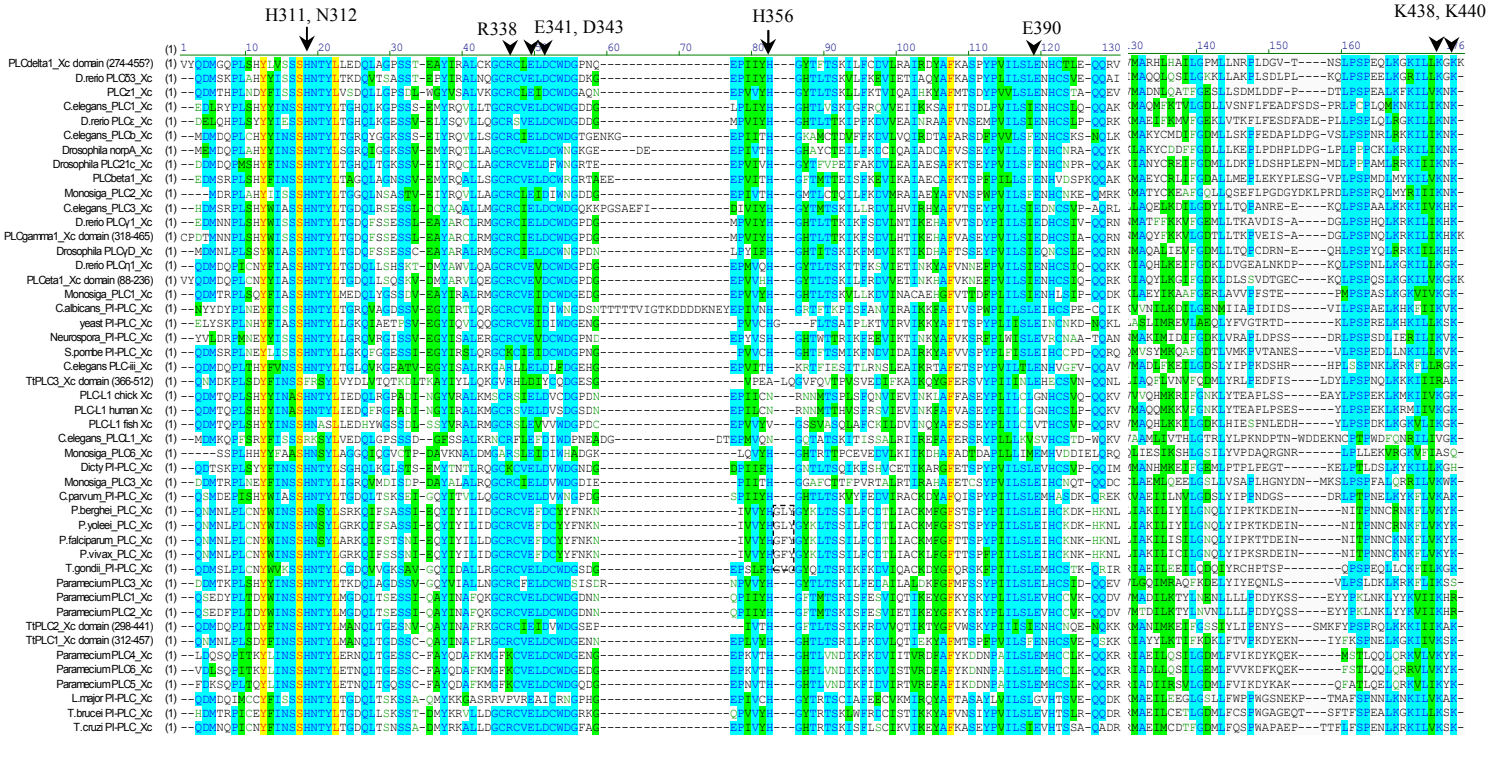


**Supplemental Fig. 2C.** Sequence alignment of the PLCXc domains from eukaryotic PLCs. Accession numbers for PLCs are listed in Supplemental Table 2. Domain boundaries were retrieved from the SMART database. The alignment was modelled on the PI-PLCδ1 PLCXc domain (ref. 17 in the manuscript). Arrows and arrowheads indicate the position of important functional amino acids: H311 and H356 are the catalytic His residues; N312, E341, D343 and E390 serve in $Ca^{2+}$ ligation and stabilization; K438 and K440 serve as salt bridges to the 4- and 5-phosphates of Ins(1,4,5)$P_3$; R338 provides barrel stabilization (ref. 17 in manuscript, numbering refers to rat PI-PLCδ1). Note that: (i) the H311/N312 motif of TtPLC3/PRIP and *C. elegans* PLC-L is not conserved (see Fig. 5D for details); (ii) the alignment of the H356 residue (HG motif) is distorted due to unique GF/LY insertions in *Plasmodia* PLCs (dotted box); (iii) all functional amino acids are conserved in almost all PI-PLCs. Marked exceptions are the PRIP/PLC-L proteins (see Fig. 5D) and *Leishmania major* PI-PLC which lacks several $Ca^{2+}$-interacting residues.

**Fig. S2 (continued)**

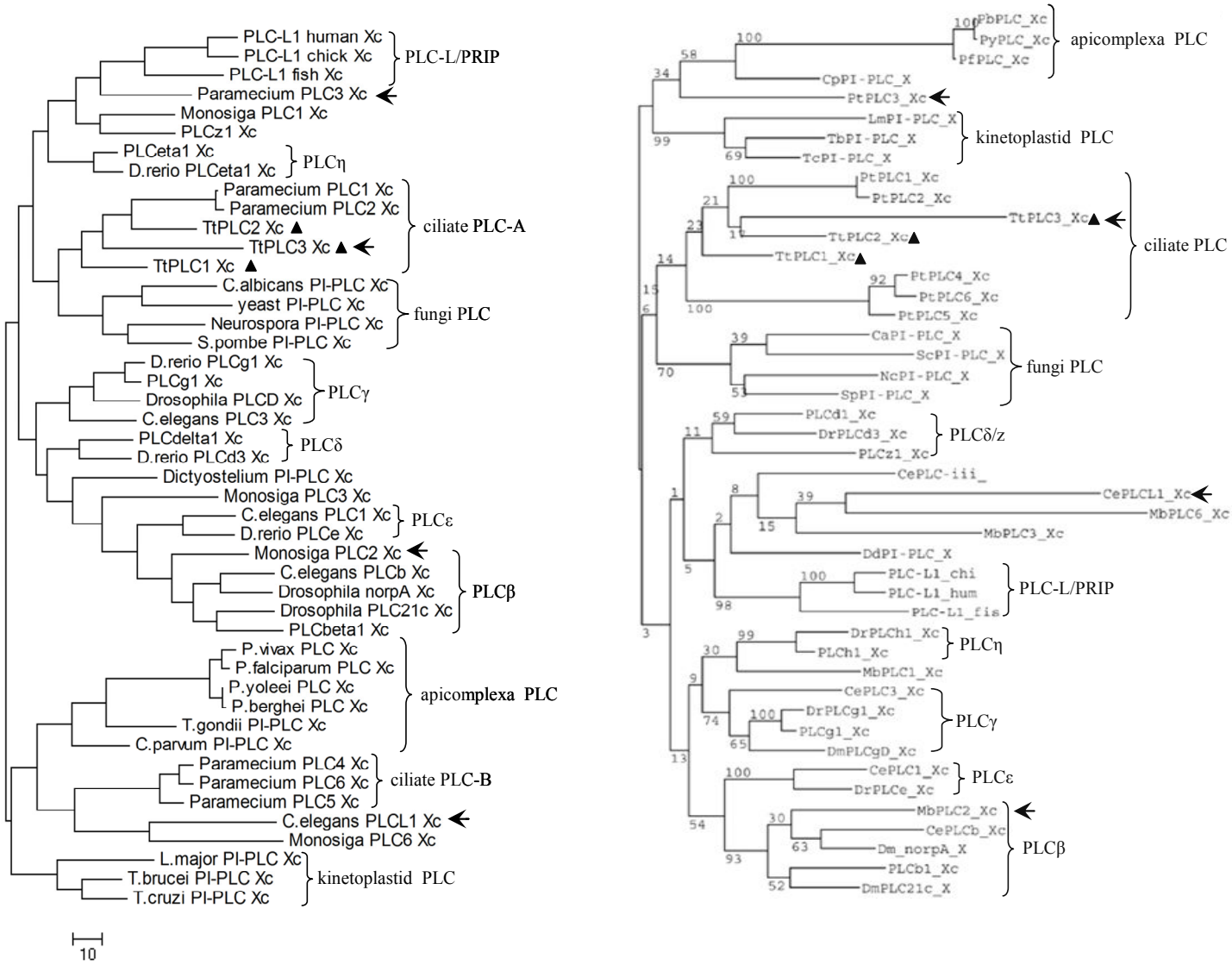


**Supplemental Fig. 2D.** Maximum parsimony (MP, left) and maximum likelihood-based (ML, right) unrooted trees of eukaryotic PLCs. Bootstrap values from 100 replicates are indicated near corresponding branches in the ML tree. Black triangles: *Tetrahymena PLC1-3*. Arrows correspond to Tt *PLC3*/*PRIP*, *Paramecium* PLC3 (PtPLC3 in ML tree), *C. elegans* PLC-L (CePLCL1 in ML tree) and *Monosiga* PLC2 (MbPLC2 in ML tree). Note that (i) Tt*PRIP* is grouped with other ciliate PLCs in both MP and ML trees and not with the PLC-L group, clearly suggesting a ciliate origin; (ii) similarly, *C. elegans* PLC-L1 is not grouped with vertebrate PLC-Ls in both MP and ML trees. Apparently, there is no direct phylogenetic relationship of TtPLC3/PRIP and *C. elegans* PLC-L1 with verterbrate PLC-L/PRIP genes and this is suggestive of convergent evolution on a specific aspect of PLC signaling pathways in these organisms. (iii) *Paramecium* PLC3 is apparently a divergent ciliate PLC while *Paramecium* PLC4-6 constitute a distinct subgroup of ciliate PLCs (see also ref. 25 in the manuscript); (iv) Significant bootstrap support values were obtained for most metazoan PLC isoforms but not for ciliate or other unicellular PLCs with the exception of *Monosiga* PLC2 that apparently is most related to PLCβ (see also Fig. 5C in the manuscript). The MP tree was constructed using the MEGA 4 software and the ML tree was constructed with the PhyML v3.0 programm at http://mobyle.pasteur.fr, using the JTT model of amino acids substitution.

**Fig. S3**

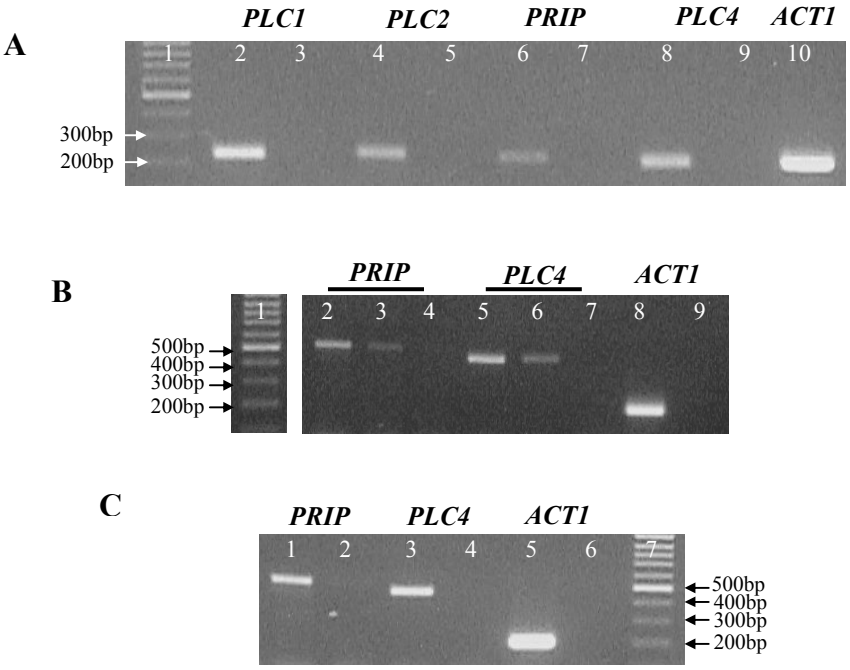


**Supplemental Fig. 3**. Expression of *PLC1*, *PLC2, PLC3*/*PRIP and PLC4* in *T. pyriformis*. Total mRNA was isolated from *T. pyriformis* strain W cells, and subjected to reverse transcription, and cDNA was amplified with the *T. thermophila* PLC-specific primers as described in Materials and Methods. (A) Lane 1 shows the results of electrophoresis of DNA size markers and lanes 3, 5, 7, 9 and 11 show the results of reactions in the absence of cDNA. All PCR products had the expected size as compared to their respective *T. thermophila* genes. Note that, in contrast to *T. thermophila* PLC genes (Fig. 6A and B in the manuscript), *PRIP* appears to be less abundant than *PLC2* in *T. pyriformis.* (B and C) A second set of primers for *PLC3/PRIP* and *PLC4* (as an additional control) with predicted PCR products of 528 and 472bp, respectively, were used with positive results in reactions with *T. thermophila* (B) and *T. pyriformis* (C) cDNA. In B, lanes 4, 7 and 9 show the results of reactions in the absence of cDNA, whereas lanes 3 and 6 show the results of reactions which utilized lesser amounts of cDNA compared to lanes 2 and 5. In C, lanes 2, 4 and 6 show the results of reactions in the absence of cDNA. In all cases, *ACT1* expression was used as control. Additional primers used were: *PLC3β* forward, 5′-TGCGATAAACAATGGTGGAA-3; *PLC3β* reverse, 5′-TTTGCAGTCGATGAGAGGAG-3 (this pair amplifies part of exon 7 of *PLC3* coding for the PLCYc domain); *PLC4β* forward, 5′-GCTCGTAAACAGCTTTGATCC-3′; *PLC4β* reverse, 5′-CGGTAATCCGAGCTGCTATC-3. Direct sequencing of the *T. pyriformis PLC1* and *PLC3*/*PRIP* PCR products in A and C resulted in unambiguous sequences of 160 bp and 416 bp, respectively, which perfectly matched with *T. thermophila PLC1* and *PRIP* respective regions coding for part of the C2 domain (*PLC1*) and the PLCYc domain (*PRIP*), as expected. Sequences have been deposited in GenBank with accession numbers HQ317216 and HQ317217.

**Fig. S4**

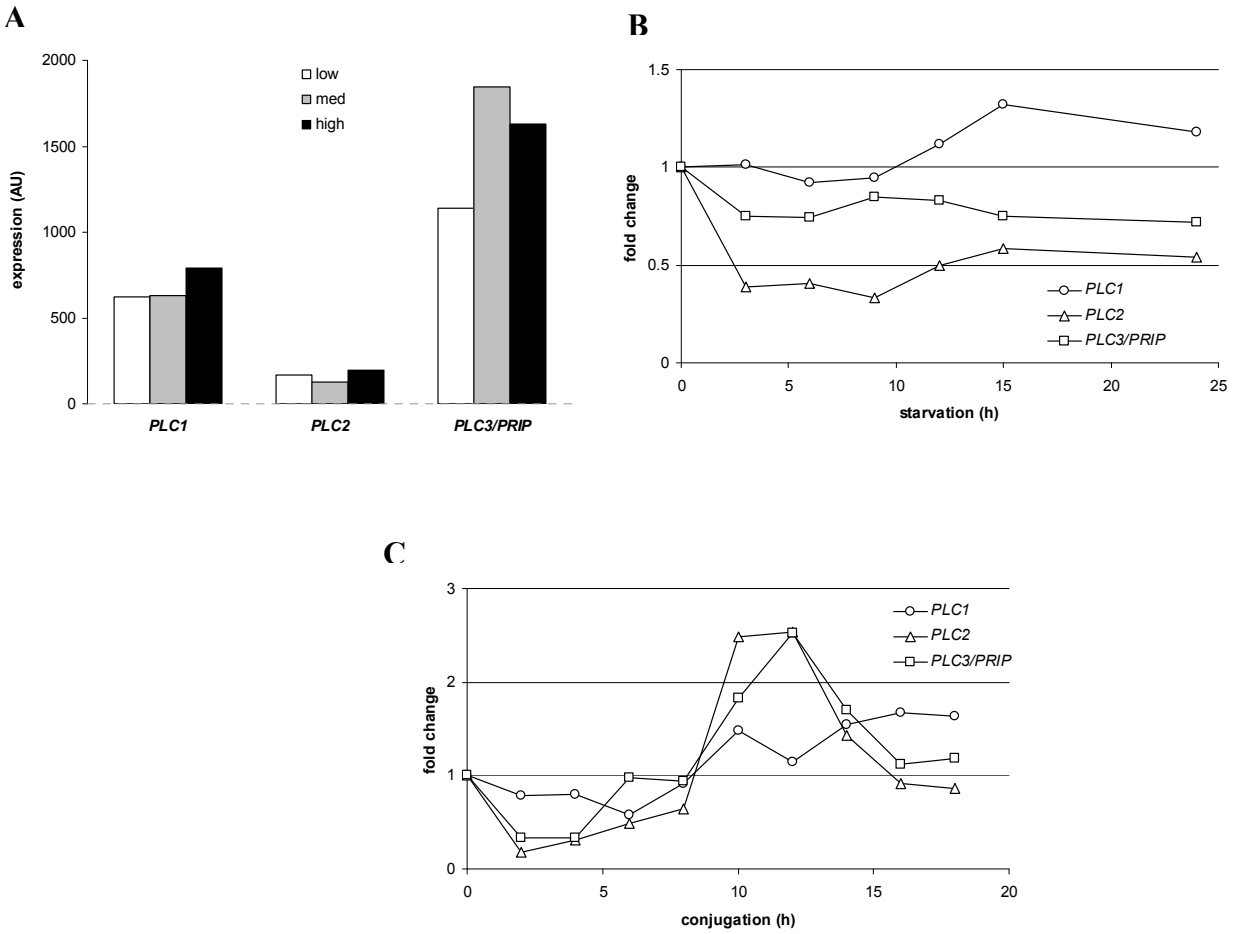


**Supplemental Fig. 4.** Differential expression patterns of Tt*PLC1* (TTHERM_00486470), Tt*PLC2* (TTHERM_00238850) and Tt*PRIP* (TTHERM_00085110) throughout growth, starvation and conjugation. Expression data for *T. thermophila* PLCs were extracted from the TGED database (http://tged.ihb.ac.cn/) and replotted in order to compare the expression at three different conditions: low, medium (med) or high cell density during growth (A), starvation (B) and conjugation (C). AU, arbitrary units. Note that, according to the study of Miao et al. (ref. 33 in the manuscript), 200 AU correspond to a level of 2x background signal. For starvation and conjugation, values are shown as fold changes relative to controls (time 0).

**Supplemental Table 1** *Tetrahymena thermophila* putative phospholipase C genes.

| Locus tag | Gene name | Genomic scaffold | Exons/ Introns *[2] | Domains (aa) *[3] | E value *[4] |
|---|---|---|---|---|---|
| TTHERM_00486470 | *PLC1* | Scf_8254527 | 4/3 | EFh (145-173/181-209)<br>PLCXc (312-457)<br>PLCYc (714-831)<br>C2 (849-959) | 1.4e+00/1.0e-02<br>1.6e-72<br>6.3e-26<br>2.4e-13 |
| TTHERM_00238850 | *PLC2* | Scf_8254373 | 4/3 | EFh (143-171/179-207)<br>PLCXc (298-441)<br>PLCYc (563-681)<br>C2 (719-826) | 1.6e+01/8.9e-01<br>1.6e-70<br>2.9e-34<br>2.3e-10 |
| TTHERM_00085110 | *PLC3/PRIP* | Scf_8254697 | 7/6 | PH (63-168)<br>EFh (251-328)<br>PLCXc (366-512)<br>PLCYc (978-1081)<br>C2 (1102-1253) | 2.4e-01<br>2.6e-02<br>6.4e-31<br>1.4e-06<br>7.9e-05 |
| TTHERM_00317320 | *PLC4* *[1] | Scf_8254548 | 1/- | PLCXc (1-82)<br>PLCYc (461-574)<br>C2 (633-731) | 5.6e-06 (Pfam database)<br>3.4e-03<br>1.9e-13 |
| TTHERM_00426140 | *BPLC1* | Scf_8254671 | 3/2 | PLCXc (45-182, 386-528) | 3.0e-19/3.0e-20<br>(SCOP database; d2plc entry) |
| TTHERM_00348190 | *BPLC2* | Scf_8254460 | 2/1 | PLCXc (1-127) | 9.0e-10<br>(SCOP database; d2plc entry) |

*[1] TTHERM_00317320 (*PLC4)* has been annotated as C2-domain containing protein
*[2] *PLC1* and *PLC2* share a common gene structure
*[3] Domain boundaries were retrieved by the SMART database
*[4] E-values were retrieved by the SMART (or PFAM or SCOP (http://supfam.cs.bris.ac.uk/SUPERFAMILY/function.html) databases where indicated). All domains were also positively identified by the NCBI conserved domain search tool.

**Supplemental Table 2** Eukaryotic and bacterial PLC genes from selected organisms.
Listed are the accession numbers and origin of PLCs used for sequence alignments and phylogenetic tree construction. *Monosiga* and *Paramecium* PLC genes were numbered arbitrarily. *Paramecium* PLCs as classified by Kloppel et al., 2009 (ref. 25 in the manuscript) are also shown in parentheses. The PLCXc domains of each protein were retrieved from the SMART database.

| Organism/Gene | Accession number |
|---|---|
| **Eukaryotic PLCs** | |
| *Candida albicans* PI-PLC | O13433.1 |
| *Neurospora crassa* PI-PLC | CAE76127.1 |
| *Saccharomyces cerevisiae* PI-PLC | CAA98004.1 |
| *Schizosaccharomyces pombe* PI-PLC | NP_594734.1 |
| *Plasmodium falciparum* PI-PLC | XP_001347417.2 |
| *Plasmodium berghei* PI-PLC | XP_679069.1 |
| *Plasmodium yoelii* PI-PLC | XP_725186.1 |
| *Plasmodium vivax* PI-PLC | XP_001614446.1 |
| *Cryptosporidium parvum* PI-PLC | XP_625844.1 |
| *Toxoplasma gondii* PI-PLC | AAV70738.1 |
| *Dictyostelium discoideum* PI-PLC | XP_629476.1 |
| *Trypanosoma cruzi* PI-PLC | XP_818111.1 |
| *Leishmania major* PI-PLC | XP_001683319.1 |
| *Trypanosoma brucei* PI-PLC | XP_828672.1 |
| *Paramecium* PLC1 (PtPLC3) | XP_001428421.1 |
| *Paramecium* PLC2 (PtPLC5) | XP_001426739.1 |
| *Paramecium* PLC3 (PtPLC1) | XP_001438852.1 |
| *Paramecium* PLC4 (PtPLC4) | XP_001428509.1 |
| *Paramecium* PLC5 (PtPLC2) | XP_001432600.1 |
| *Paramecium* PLC6 (PtPLC6) | XP_001426835.1 |
| *Monosiga brevicollis* PLC1 | XP_001750272.1 |
| *Monosiga brevicollis* PLC2 | XP_001743113.1 |
| *Monosiga brevicollis* PLC3 | XP_001750624.1 |
| *Monosiga brevicollis* PLC4 | XP_001743126.1 |
| *Monosiga brevicollis* PLC5 | XP_001747504.1 |
| *Monosiga brevicollis* PLC6 | XP_001747624.1 |
| *Danio rerio* PLC delta 3 | NP_001092893.1 |
| *Danio rerio* PLC eta 1 | XP_694841.2 |
| *Danio rerio* PLC gamma 1 | NP_919388.1 |
| *Danio rerio* PLC epsilon 1 | NP_001155125.1 |
| *Caenorhabditis elegans* PLC-3 | NP_496205.2 |
| *Caenorhabditis elegans* PLC beta | AF188477_1 |
| *Caenorhabditis elegans* PLC-1 | NP_001024619.1 |
| *Caenorhabditis elegans* PLC-L1 | NP_741068.1 |
| *Drosophila melanogaster* PLCg D | BAA06189.1 |
| *Drosophila melanogaster* PLC21c | NP_995606.1 |
| *Drosophila melanogaster* norpA | NP_001014720.1 |
| *Homo sapiens* PLC-like 1 | NP_006217.3 |
| *Gallus gallus* PLC-L | XP_421916.2 |
| *Danio rerio* PLC-L2 | XP_701253.3 |
| *Homo sapiens* PLC gamma 1 | ABB84466.1 |
| *Homo sapiens* PLC beta 1 | AAF86613.1 |
| *Homo sapiens* PLC delta 1 | AAA73567.1 |
| *Homo sapiens* PLC, eta 1 | EAW78747.1 |
| *Homo sapiens* PLCz1 | Q86YW0.1 |

| Organism/Gene | Accession number |
|---|---|
| **Bacterial PLCs** | |
| *Bacillus cereus* PtdIns-PLC | P14262.1 |
| *Trypanosoma brucei* GPI-PLC | AAX79015.1 |
| *Trypanosoma cruzi* GPI-PLC | O15886.1 |
| *Homo sapiens* PLCXD2 | EAW79695.1 |
| *Homo sapiens* PLCXD1 | EAW66822.1 |
| *Drosophila melanogaster* RE10196p | AAL90315.1 |
| *Dictyostelium discoideum* DDB_G0293730 | Q54BH5.2 |
| *Entamoeba dispar* PtdIns-PLC | EDR29964.1 |
| *Yersinia mollaretii* PtdIns-PLC | ZP_04642139.1 |
| *Listeria monocytogenes* PtdIns-PLC | ACM43701.1 |
| *Candida albicans* PtdIns-PLC | CAB92911.1 |